Esterase-Like Activity of Serum Albumin: Characterization of Its Structural Chemistry Using p-Nitrophenyl Esters as Substrates

Yuji Sakurai,[1] Shen-Feng Ma,[1] Hiroshi Watanabe,[1] Noriyuki Yamaotsu,[2] Shuichi Hirono,[2] Yukihisa Kurono,[3] Ulrich Kragh-Hansen,[4] and Masaki Otagiri[1,5]

Received September 21, 2003; accepted October 10, 2003

Purpose. To elucidate the catalytic mechanism of the esterase-like activity of serum albumin (SA), the reactivity of SA from six species was investigated using *p*-nitrophenyl esters as model substrates.
Methods. The effect of pH and the energetic and thermodynamic profiles of SA were determined for all species for *p*-nitrophenyl acetate (PNPA). Then, kinetic and thermodynamic studies using a series of *p*- and *o*-nitrophenyl esters with different side chains and human SA (HSA) were carried out. The influence of deuterium oxide was also evaluated. Finally, the information gained was used to construct a computer model of the structural chemistry of the reaction.
Results. The pH profiles suggest that the nucleophilic character of the catalytic residue (Tyr-411 in the case of HSA) is essential for activity. This k_{cat}-dependent activity was found to increase with a decrease in the activation free energy change (ΔG). Hence, the magnitude of ΔG, which is dependent on activation entropy change (ΔS), as calculated from the thermodynamic analysis, can be regarded as an indicator of hydrolytic activity. It indicates that *p*-nitrophenyl propionate (PNPP) is the best substrate by evaluating the reactions of nitrophenyl esters with HSA. The findings here indicate that deuterium oxide has no significant effect on the rate of hydrolysis of PNPA by HSA.
Conclusions. The results are consistent with a scenario in which HSA becomes acylated due to a nucleophilic attack by Tyr-411 on the substrate and then is deacylated by general acid or base catalysis with the participation of water.

KEY WORDS: esterase-like activity; *p*-nitrophenyl esters; serum albumin; species difference; structure–activity relationship.

INTRODUCTION

As the most abundant soluble protein in the body (about 4% in serum) and the most prominent protein in plasma, serum albumin (SA) is responsible for a multiplicity of functions, including the maintenance of blood osmolarity, acting as an antioxidant, and serving as a solubilizing agent and carrier for many endogenous and exogenous compounds (1). It is also well-known that it is a major binding protein for the transport of a large number of drugs (1).

Studies of SA have also revealed the important role of this protein as a catalyst for the hydrolysis of various compounds, such as esters, amides, and phosphates (2,3). Ikeda et al. reported that the most prominent catalytic, esterase-like, active sites of human serum albumin (HSA) are closely related to its drug binding sites, because various drugs inhibit this activity (4). Thus, the active site of HSA with respect to *p*-nitrophenyl acetate (PNPA) is thought to be the same as the binding site for several benzodiazepines (site II), and the enzymatic active site with respect to nitroaspirins is in close proximity to the warfarin binding site (site I) (4). However, in spite of the extensive literature on these reactive sites, their properties and their differences among species are not known in detail.

Typically, the esterase activity (e.g., carboxylesterase activity) is more pronounced in plasma from primates than in other animals such as dogs, rabbits, snakes, and fish (5,6). The esterase-like activity of SA has been reported to be highest in human and is completely absent in SA from horse (Order Perissodactyla) (1,7). The primary structure of several species of albumin is now known (1), and mammalian types show amino acid sequence identities of about 70–80%. Therefore, it is conceivable that they have comparable three-dimensional structures. In fact, X-ray diffraction studies by Ho et al. showed that the crystal structure of horse albumin is similar to the three-dimensional structures of HSA (8,9). Studies involving site-directed mutagenesis have shown that Arg-410 and, especially, Tyr-411 are important for the esterase-like activity of HSA (10). However, many albumin species, including horse albumin, also contain arginine and tyrosine in the same or corresponding positions, but have different enzymatic activities (1). Therefore, other, and presently unknown, factors must be important as well.

In the current study, we report on a detailed examination of the esterase-like activity of albumin and the mechanism of the catalytic reaction. Species differences were first examined. This involved a determination of pH profiles and the collection of thermodynamic data on the esterase activity of SA from human, bovine, dog, rabbit, rat, and horse using PNPA as a substrate. To characterize the structural chemistry of the active site, hydrolytic reactions of a series of *p*-nitrophenyl and *o*-nitrophenyl esters with HSA were also investigated. Finally, the optimum structure of the substrate–HSA complex was constructed using the X-ray structure of the HSA:myristate (MYR):*tri*-iodobenzoic acid (TIB) complex.

MATERIALS AND METHODS

Materials

HSA was a gift from the Chemo-Sera-Therapeutic Research Institute (Kumamoto, Japan), and dog, rabbit, bovine, horse, and rat serum albumin samples were purchased from the Sigma Chemical Co. (St. Louis, MO, USA). All of the albumin samples were defatted according to Chen's method before use (11).

[1] Graduate School of Pharmaceutical Sciences, Kumamoto University, Kumamoto 862-0973, Japan.
[2] The School of Pharmaceutical Sciences, Kitasato University, Tokyo 108-8641, Japan.
[3] Faculty of Pharmaceutical Sciences, Nagoya City University, Nagoya 467-8603, Japan.
[4] Department of Medical Biochemistry, University of Aarhus, Aarhus C DK-8000, Denmark.
[5] To whom correspondence should be addressed. (e-mail: otagirim@gpo.kumamoto-u.ac.jp)

ABBREVIATIONS: Arg, arginine; HSA, human serum albumin; MD, molecular dynamics; MYR, myristate; PNPA, *p*-nitrophenyl acetate; PNPE, *p*-nitrophenyl esters; PNPP, *p*-nitrophenyl propionate; SA, serum albumin; TIB, *tri*-iodobenzoic acid; Tyr, tyrosine.

0724-8741/04/0200-0285/0 © 2004 Plenum Publishing Corporation

PNPA, *p*-nitrophenol, *o*-nitrophenyl acetate, and *o*-nitrophenol were purchased from Nacalai Tesque (Kyoto, Japan), and other *p*-nitrophenyl esters were ordered from Sigma Chemical Co. Deuterium oxide (D > 99.75%) was obtained from Merck Co. (Darmstadt, Germany). All other chemicals were of analytical grade.

Procedures for Kinetic Runs

The buffer systems used were as follows: pH 6.0–8.5, 1/15 M phosphate; pH 9.0–10.5, 1/20 M borate. The ionic strength of each buffer was not fixed, because the addition of NaCl to the buffer decreased the reaction rates in a complicated manner (12). The reaction medium contained 0.5% (v/v) acetonitrile. The temperature was 25°C except for the thermodynamic analysis, which was done in a range of 15~35°C.

Hydrolysis of substrate (5 μM) by various species of albumin (at least a 5-fold excess concentration over the substrate) was carried out in such a way that complications by any multiple reactive sites of albumin were avoided. It is said that the substrates preferentially reacted with the primary reactive site of albumin under these conditions (12,13). The reactions were followed with a stopped-flow spectrophotometer (Otsuka Electronics Co. Ltd., Osaka, Japan) at 400 nm by monitoring the appearance of the corresponding phenol. Under these conditions, pseudo-first-order rate constants could be obtained.

Measurement of Reaction Parameters

The reactions of the substrates with albumin are assumed to proceed through the pathway shown in Fig. 1 (4). In this chart, PNPE is the substrate and EST–Alb denotes the Michaelis–Menten type complex between EST and albumin. Acyl-Alb denotes albumin acylated by the substrate, and K_S represents the dissociation constant of the complex. The rate constants of EST–Alb are represented by k_{cat} and k_0, respectively. k is the rate constant for the dissociation of Acyl-Alb.

The pseudo-first-order rate constant for the release of phenol, k_{obs}, can be represented as follows:

$$k_{obs} = \frac{k_0 K_S + k_{cat}[\text{albumin}]}{K_S + [\text{albumin}]} \quad (1)$$

Here, [albumin] is the concentration of albumin. Because the value of k_{cat} is much larger than that of k_0 (2000- to 6000-fold), so k_0 can be ignored (4). The K_S and k_{cat} values can be calculated from the intercept and slope of a double-reciprocal plot using Eq. (2):

$$\frac{1}{k_{obs}} = \frac{K_S}{k_{cat}[\text{albumin}]} + \frac{1}{k_{cat}} \quad (2)$$

Determination of pK_a

Assuming that the hydrolytic reaction catalyzed by albumin is dependent on the ionic form of Tyr-411, the rate of the reaction should be both the ionization constant (K_a) and pH-dependent, as described in Eq. (3):

$$\left(\frac{k_{cat}}{K_S}\right)_H = \left(\frac{k_{cat}}{K_S}\right) K_a \times \frac{1}{K_a + [H^+]} \quad (3)$$

Equation (3) has the same form as the Michaelis–Menten equation, where k_{cat}/K_S is the value at completely ionized Tyr form, and $(k_{cat}/K_S)_H$ is the measured value at a given $[H^+]$. K_a can be calculated as follows, where $[H^+]$ is the hydrogen ion concentration.

$$\left(\frac{k_{cat}}{K_S}\right)_H = \left(\frac{k_{cat}}{K_S}\right) - \left(\frac{k_{cat}}{K_S}\right)_H [H^+] \times \frac{1}{K_a} \quad (4)$$

The pK_a values were obtained using least squares method.

Thermodynamic Analysis

The free-energy change for an enzymatic reaction has generally been discussed according to the literature (14). Each free-energy parameter was calculated using Eqs. (5), (6), and (7), where ΔG_S is the free-energy change for the initial reaction of the enzyme and substrate, ΔG the activation free energy for the rate-determining step, ΔG_T the free-energy difference for the reaction, R the gas constant, T the absolute temperature, k_B the Boltzmann constant, and h the Planck constant.

$$\Delta G_S = -RT\ln(1/K_S) \quad (5)$$

$$\Delta G = RT\{\ln(k_B T/h) - \ln k_{cat}\} \quad (6)$$

$$\Delta G_T = \Delta G - \Delta G_S \quad (7)$$

The thermodynamic investigation of the albumin-catalyzed reaction was performed in the temperature range 15~35°C. The activation energy (E_a) was obtained from an Arrhenius plot of the rate constant vs. temperature following Eq. (8).

$$\frac{d \ln k_{cat}}{d\,(1/T)} = \frac{E_a}{R} \quad (8)$$

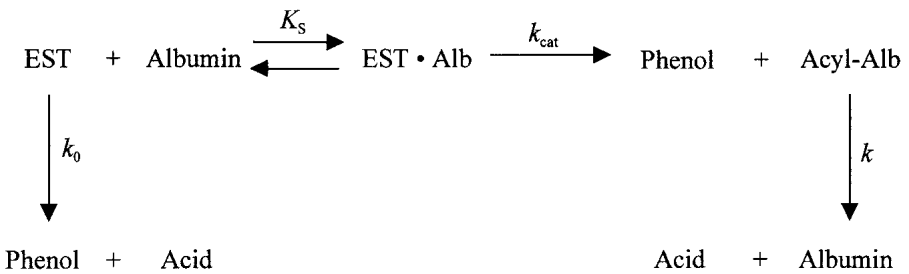

Fig. 1. Spontaneous and albumin (Alb) catalyzed hydrolysis of *p*-nitrophenyl esters (EST).

The activation enthalpy change (ΔH) and the activation entropy change (ΔS) were calculated using Eqs. (9) and (10), respectively.

$$\Delta H = E_a - RT \quad (9)$$

$$\Delta S = (\Delta H - \Delta G)/T \quad (10)$$

Conformational Analysis of PNPP

The conformational analysis of PNPP was performed using the CAMDAS 2.1β2 program (15). Ten molecular dynamics (MD) calculations were simultaneously performed using different initial structures. Each of the MD calculations was carried out for 600 ps with an integral time step of 1 fs. The lengths of the covalent bonds were fixed. The temperature of the system was maintained at 900 K in order to enhance the sampling efficiency. The Tripos force field (16) was used to evaluate the potential energy surface of the molecule. The electrostatic and hydrogen bonding term of the potential were ignored in order to avoid intramolecular hydrogen bonding. The angle and torsional terms of the potential were reduced by a factor of 0.8 in order to increase the flexibility of the molecule. Conformers were sampled at 100 step intervals, thus producing 6000 conformations for each MD calculation. A total of 60,000 conformations were preclustered with an root mean square deviation (rmsd) threshold of 0.2 Å. Superposition and rmsd calculations were performed for all of the heavy atoms. After sampling, the reclustering of the sampled conformers was performed with an rmsd threshold of 0.2 Å. Before the clustering, each conformer was minimized until the root mean square of the potential energy gradients was below 0.005 kcal mol^{-1} $Å^{-1}$. Finally, 723 conformers were obtained.

Preparation of HSA Template

To obtain the HSA template structure for docking, we used the crystal structure of the HSA:myristate (MYR):*tri*-iodobenzoic acid (TIB) complex (PDB ID code: 1bke) (17). Due to the lack of *N*-terminal residues from the 1st to the 3rd and of the *C*-terminal residue of the 585th in the PDB structure, we treated the 4th residue as the *N*-terminus and the 584th residue as the *C*-terminus. The initial positions of the other missing atoms in the PDB structure were generated using the SYBYL 6.6.2 program package (18). The Tripos force field was used. The AMBER 1991 charges (19) were used as the charges for HSA. Gasteiger-Hückel (20–23) charges were used as the charges for MYR and for TIB. Only the missing atoms were minimized using SYBYL to below 0.05 kcal mol^{-1} $Å^{-1}$ for the root mean square of the gradients. The cut-off distance for nonbonded interactions was 8 Å. Finally, the MYR and TIB molecules on HSA were deleted.

Docking of PNPP with HSA

The docking calculation of each PNPP conformation with HSA was performed using the UNITY 4.1.2 program package (24). A MOLCAD fast Connolly surface was created for the protein atoms surrounding site II of HSA (within 8 Å from MYR-1003 and MYR-1004). We defined a UNITY surface volume constraint expanded by a tolerance of 1.0 Å from the MOLCAD surface. The PNPP molecule should be the inside of the surface volume constraint. Hydrogen bond donors in protein atoms surrounding site II were defined as UNITY queries. However, this was not done for hydrogen bond acceptors because there are no donors in PNPP. The PNPP molecule should form a hydrogen bond to Arg-410, which is important for esterase-like activity (10), and to at least one of the other residues. However, Tyr-411 was not included in the UNITY queries because it is a catalytic residue. A hydrogen bond tolerance was set within 0.5 Å. We searched for conformers that satisfied the above conditions using a UNITY 3D Search and obtained only one hit. In this search, the HSA template and each PNPP conformer were kept rigid. Finally, the docked HSA–PNPP complex was minimized in a same manner as above. AM1-Wang-Ford charges (25,26) were generated as charges for the PNPP using CS MOPAC (27).

RESULTS AND DISCUSSION

Species Differences in Esterase-Like Activity

pH Profiles

The pH profiles for $k_{cat,}$ K_S, and k_{cat}/K_S for the hydrolysis of PNPA by the different types of SA were constructed. The k_{cat} values are markedly dependent on pH in all species examined (data not shown) and show that the susceptibility of the active sites to nucleophilic attack increases with pH. In contrast, the K_S values decrease with increasing pH (data not shown). It has been reported that pH-dependent conformational changes (N–B transition) occur in albumin when going from neutral to slightly alkaline pH (28). Therefore, alterations in nucleophilic attack in active sites and in the affinity to PNPA could be due, totally or partly, to changes in the tertiary structure of albumin, which accompany the pH-dependent N–B transition. The k_{cat}/K_S values increase with raising pH (data not shown). This difference in activity appears to be mainly due to differences in k_{cat}.

The results of the pH experiments indicate that nucleophilicity in the active sites is very important in catalysis activity. The pK_a value for the hydrolysis of PNPA with various albumins is calculated, and the result for human is shown in Fig. 2, as a typical example. It is lowest in human albumin, in which, however, the highest enzymatic activity was found. Horse albumin has the highest pK_a value for hydrolysis but has the lowest enzymatic activity (Table I). These results indicate that hydrolytic activity is dependent on the pK_a and on the nucleophilicity of the most important catalytic residue, Tyr-411, in the various albumins. According to X-ray crystallographic studies of HSA, the oxygen of the hydroxyl group of Tyr-411 is adjacent to the nitrogen of the guanidine group of Arg-410 (10). Therefore, the species differences in esterase-like activity could be affected by structural changes after substrate binding.

On the other hand, Tyr-411 and Arg-410, which are essential for hydrolytic activity, are perfectly preserved in all species examined to date, and the amino acid residues in the immediate vicinity of Tyr-411 residue are highly conserved among species. Thus, the significant decrease in reactivity in rat and horse albumin must reflect differences in the microenvironment in the active sites rather than a deficiency of basic activity. The SA with a lower pK_a can cause an easier

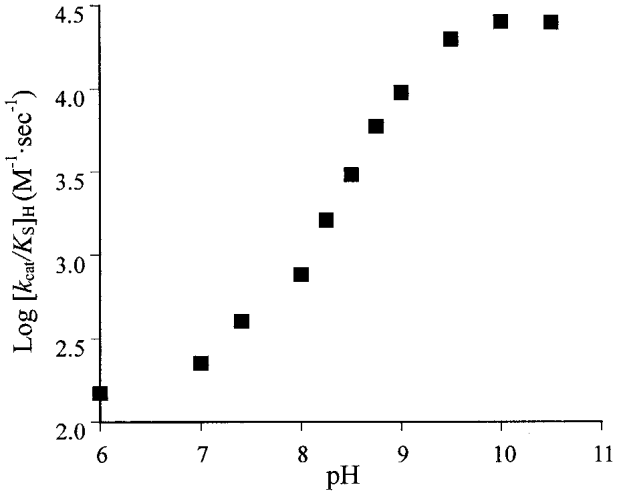

Fig. 2. Plots of [log k_{cat}/K_S]$_H$ against pH for the hydrolytic reaction of PNPA with HSA. Reaction conditions: 1/15 M phosphate buffer at 25°C. Plots represent mean ± SD (n = 3).

dissociation of Tyr-411 residue, which can be predicted to have a higher reactivity in consequence.

Energy and Thermodynamic Profiles

Using the hydrolysis parameters, we calculated the energy changes for the different albumins at pH 7.4. ΔG_T, considered to be an indicator of the energy difference, is dependent on ΔG and can be calculated from k_{cat} (Table II). As described above, the hydrolysis reaction of albumin is k_{cat} dependent. This observation suggests that the esterase activity is due to the energy difference between the substrate–protein complex in the transition state (ES*) and in the ground state (ES).

The free-energy diagram for the hydrolysis of human and horse albumins toward PNPA is given in Fig. 3. The different esterase-like activity of various albumins is due to differences in ΔG, namely, the extent of stabilization of the transition state.

In order to investigate the characteristic feature of hydrolysis with respect to PNPA in greater detail, thermodynamic studies on this catalytic reaction were performed. As given in Table II, ΔG, mentioned above, which reflects the activity difference, is due to an entropy change (ΔS). Hence, the entropic difference between the ground state and the transition state is especially significant for hydrolytic reactions of albumin. The active site of HSA to which the substrate binds, having a perfect orientation to the binding site of the substrate (the ester portion) for the hydrolysis, shows a smaller difference in entropy between the transition state and the ground state. This is the reason why hydrolysis by HSA proceeds more readily than by the other albumins. Otherwise, the entropic difference can be also explained by the differences in the effects on water structure in active site(s).

Table I. pK_a Values for the Catalytic Group in Various Albumins

Species	pK_a
Human	9.2
Bovine	9.3
Rabbit	9.4
Dog	9.4
Rat	9.5
Horse	9.7

Average of values from 2–3 experiments, which coincided with each other within 2%.

Table II. Free Energy and Other Thermodynamic Parameters for the Hydrolysis of PNPA by Various Albumins*

Species	ΔG_T (kcal/mol)	ΔG_S (kcal/mol)	ΔG (kcal/mol)	ΔH (kcal/mol)	$T\Delta S$ (kcal/mol)
Human	13.9	–5.0	18.9	15.8	–3.2
Bovine	14.5	–4.6	19.1	15.3	–3.9
Rabbit	14.6	–4.6	19.2	15.0	–4.2
Dog	14.9	–4.8	19.7	15.3	–4.4
Rat	15.5	–5.1	20.6	14.8	–5.7
Horse	15.7	–5.1	20.8	14.9	–5.9

PNPA, P-nitrophenyl acetate.

* Reaction conditions: 1/15 M phosphate buffer (pH 7.4) at 25°C. Average of values from two experiments, which coincided with each other within 6%.

Structure–Activity Relationships

Significant variations in hydrolytic activity were found for different substrates, even if they contained the same functional group. Structure–activity studies with enzymes have made it relatively easy to define the structure and the physicochemical features of the active sites by measuring the effects of changes in the structure of the substrate on its interaction with the enzyme (14).

In order to characterize the active site(s) of HSA toward PNPA, the reactions of *p*- and *o*-nitrophenyl esters with HSA were investigated kinetically and thermodynamically. The kinetic parameters for the hydrolytic reactions of nitrophenyl esters with HSA are listed in Table III. The values of K_S

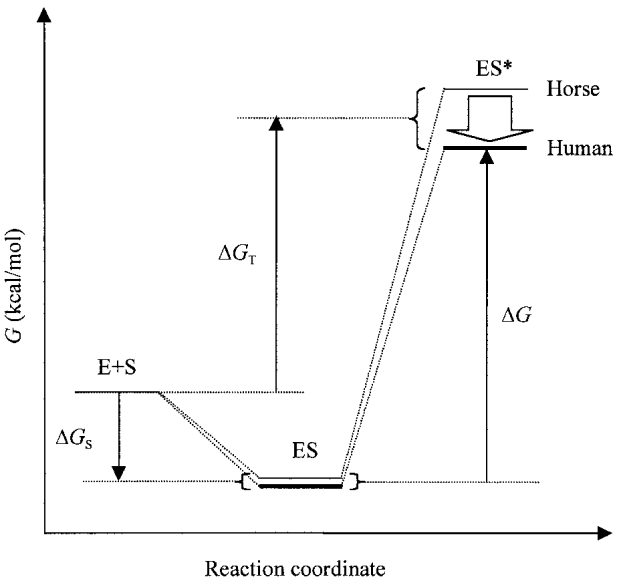

Fig. 3. Comparison of the free-energy profiles of the hydrolytic reaction of PNPA with albumin from human and horse. ΔG_T, free-energy differences; ΔG_S, free-energy change for the initial reaction of albumin and PNPA; ΔG, activation free energy.

Table III. Kinetic Parameters for the Hydrolysis of *p*- and *o*-Nitrophenyl Esters by HSA*

Substrate	Number of C in side chain	k_{cat} (10^{-3} s^{-1})	K_S (10^{-2} mM)	k_{cat}/K_S (M^{-1} s^{-1})
p-nitrophenyl ester				
PNPA	C_2	86.8 ± 4.8	21.7 ± 0.3	403.4 ± 35.6
PNPP	C_3	166.2 ± 12.2	15.5 ± 0.2	1079.3 ± 135.8
Butyrate	C_4	19.3 ± 0.8	7.5 ± 0.1	261.0 ± 23.9
Valerate	C_5	2.8 ± 0.1	4.5 ± 0.1	63.3 ± 6.2
Capronate	C_6	1.2 ± 0.1	2.3 ± 0.1	55.0 ± 19.0
Caprylate	C_8	1.1 ± 0.2	0.9 ± 0.0	133.7 ± 43.6
Caprinate	C_{10}	0.6 ± 0.0	1.0 ± 0.0	61.0 ± 14.4
Laurate	C_{12}	0.3 ± 0.0	1.3 ± 0.0	25.7 ± 6.8
Trimethyl acetate	C_5	0.4 ± 0.2	11.3 ± 0.3	3.1 ± 1.0
o-nitrophenyl ester				
Acetate	C_2	3.3 ± 0.6	10.7 ± 0.0	30.6 ± 4.6

HSA, human serum albumin; PNPA, *p*-nitrophenyl acetate; PNPP, *p*-nitrophenyl propionate.
* Reaction conditions: 1/15 M phosphate buffer (pH 7.4) at 25°C. The concentration of substrate is 5 mM and that of HSA is 25–150 mM. Each value is shown as mean ± SD. (n = 4–5).

decreased with increasing length of the side chain. Up to *p*-nitrophenyl valerate (a five-carbon side chain) a linear decrease in K_S values against the increase in the number of carbons in the side chain was found, showing that the hydrophobic side chain of the substrate influences the hydrolytic reaction. However, the decrease in k_{cat}/K_S and k_{cat} values, depending on the incremental length of the side chain, was not a decrease but a pronounced increment in the case of PNPP (a three-carbon side chain). This effect was one of affinity to albumin. Corresponding to the hydrolytic differences of the various albumins, the k_{cat}-dependent hydrolytic reaction catalyzed by albumin is due to the directing properties of binding to the substrate rather than affinity to albumin. It is conceivable that PNPP has a structure that is more suitable to the active expression of albumin, compared with other *p*-nitrophenyl esters. However, among structural isomers with the same molecular weight, such as PNPA and *o*-nitrophenyl acetate or *p*-nitrophenyl valerate and *p*-nitrophenyl trimethylacetate, substantial differences in activities were observed, which are believed to be related to steric exclusion caused by the different branches and sites of branching in the side chain.

The findings relative to the reactions of *p*-nitrophenyl esters with HSA are consistent with the above experimental studies on species differences using PNPA, suggesting that hydrolytic activity is dependent on the activation free energy (ΔG) (Table IV). Differences in the free-energy diagrams for the hydrolysis of PNPP vis-à-vis capronate can be illustrated as following the same pathway as shown in Fig. 3, where the transition state of capronate–HSA intermediate (ES*) has the highest energy of all the *p*-nitrophenyl esters. Stabilization of the transition state is an important aspect of the hydrolytic reaction, and ΔG is an indicator of the esterase-like activity of albumin. As a marker of chemical conversion, k_{cat} is more significant for hydrolytic activity than K_S, which can be thought of as an index of affinity for the substrate.

The magnitude of the activation free energy (ΔG) is related to the magnitude of the activation entropy change (ΔS) as seen from the thermodynamic analysis (Table IV). Hence, because of the entropic difference between the enzyme–substrate complex states (ES) and the transition state (ES*), PNPP has the minimum value of the related nitrophenyl ester derivatives tested and, therefore, has the highest activity in this study. That is, PNPP has an optimal structure and a more perfect orientation for binding to albumin than the other esters during the hydrolytic reaction.

Considering the findings of hydrolytic differences between various species, it can be concluded that a ΔS dependence of the transition state stabilization is significant for albumin hydrolysis and that the binding of the substrate to albumin is a contributing factor that determines activity.

Structural Mechanism of Esterase-Like Activity

The catalytic reaction of serine-proteases, a primary hydrolase, can be divided into two processes. Initially, the enzyme and substrate associate to form a noncovalent enzyme–

Table IV. Free Energy and Other Thermodynamic Parameters for the Hydrolysis of Esters by HSA*

Substrate	Number of C in side chain	ΔG_T (kcal/mol)	ΔG_S (kcal/mol)	ΔG (kcal/mol)	ΔH (kcal/mol)	$T\Delta S$ (kcal/mol)
PNPA	C_2	13.9	–5.0	18.9	15.8	–3.1
PNPP	C_3	13.3	–5.2	18.5	16.3	–2.2
Butyrate	C_4	14.2	–5.6	19.8	14.3	–5.5
Valerate	C_5	15.0	–5.9	21.0	14.7	–6.2
Capronate	C_6	15.1	–6.3	21.5	12.8	–8.7

HSA, human serum albumin; PNPA, *p*-nitrophenyl acetate; PNPP, *p*-nitrophenyl propionate.
* Reaction conditions: 1/15 M phosphate buffer (pH 7.4) at 25°C. Average of values from two experiments, which coincided with each other within 4%.

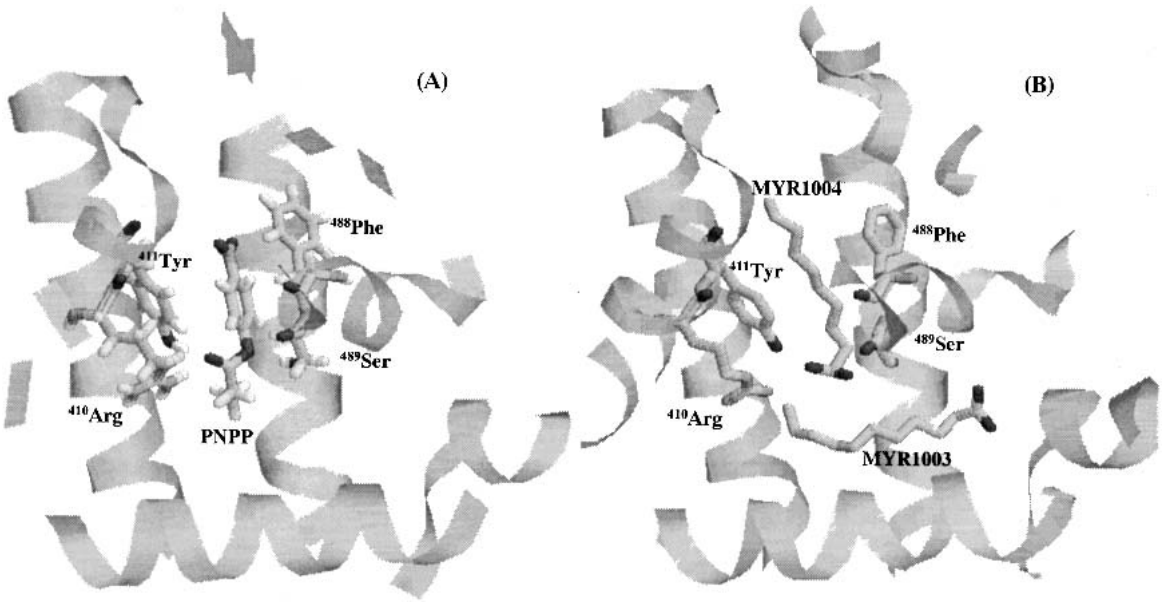

Fig. 4. Binding model for PNPP in site II of HSA (A) and the X-ray crystallographic structure of the HSA–myristate (MYR) complex in site II of HSA (B). The illustration was made with the RasMol program.

substrate complex, which is held together by interactions between the hydroxyl group of the serine residue and the substrate (referred to as a catalytic triad). This complex represents the first tetrahedral intermediate. Water is then involved in the formation of the enzyme–product complex via a second tetrahedral intermediate with the acyl-serine. This is followed by transacylation from serine to water. In addition to this catalytic triad mechanism, a region of the enzyme, termed the oxyanion hole, has been reported to exist and which promotes catalysis by providing transition-state stabilization (29).

The catalytic reaction between HSA and PNPA can be expressed quantitatively using the Michaelis–Menten equation. Means et al. reported that, after combining rapidly and reversibly into an active albumin–substrate intermediate, *p*-nitrophenol is generated and rapid acetylation occurs at the reactive residue, Tyr-411 (2). Ohta et al. observed that the second reaction, deacetylation of acetyl-albumin, is considerably slower than the first step (13). Except for these findings, little is known concerning the esterase-like activity of HSA. For example, there have been no reports concerning the possible presence of a catalytic triad or an oxyanion hole, as has been reported for serine-proteases.

In order to elucidate the detailed catalytic mechanism of the esterase-like activity of HSA, the influence of deuterium oxide on the reactivity was investigated. Subsequently, a complex of PNPP, showing the highest activity among the *p*-nitrophenyl esters tested, and HSA was constructed using computer modeling techniques.

Isotope Effect of Deuterium Oxide

The involvement of a water molecule and proton transfer can be evaluated by measurement of the deuterium oxide isotope effect (14). The influence of this molecule on the hydrolysis of PNPA by HSA was investigated to track the behavior of the proton (data not shown). The result can be regarded as a reflection of the acetylation reaction that occurs during the first step of the hydrolytic reaction, generating *p*-nitrophenol. Because no significant deuterium oxide isotope effect could be detected, this implies that a water molecule is not involved in the hydrolysis catalyzed by HSA. More specifically, the first step of the hydrolysis does not proceed via general acid or base catalysis, but is predominantly due to the nucleophilic attack of Tyr-411 residue.

The same proton exchange technique has been used to investigate the catalytic mechanism of many serine proteases (30). In these cases, the reactivity was dependent on the mole fraction of deuterium present, suggesting that the isotope effect observed for these reactions originated from the active-site serine hydroxyl group (i.e., the reactions involved the formation of catalytic triads). The current results are in contrast to these findings and imply that a catalytic triad is not involved in the hydrolysis of PNPA by HSA.

On the other hand, using *N*-trans-cinnamoylimidazoles containing amide bonds as model substrates, during the second step of hydrolysis, the deacylation rate of the cinnamoyl–albumin was found to be about 3- to 4-fold smaller in deuterium oxide than in water (13). This deuterium effect indicates that a water molecule plays a role in the deacylation reaction. Therefore, general acid or base catalysis rather than nucleophilic catalysis predominates in the deacylation of cinnamoyl–albumin. The deacetylation of acetyl-albumin, in the second step of the hydrolysis of PNPA, appears to proceed according to the same mechanism as *N*-trans-cinnamoylimidazoles.

In summary, the hydrolysis of PNPA by HSA could take place as follows: HSA is initially acetylated as the result of a nucleophilic attack of Tyr-411 on the substrate, and the deacetylation of acetyl-albumin then proceeds via general acid or base catalysis involving a water molecule.

Three-Dimensional Structure of the Modeled HSA–PNPP Complex

In the model of HSA–PNPP complex, the binding of PNPP was similar to that of MYR-1004 in the X-ray structure

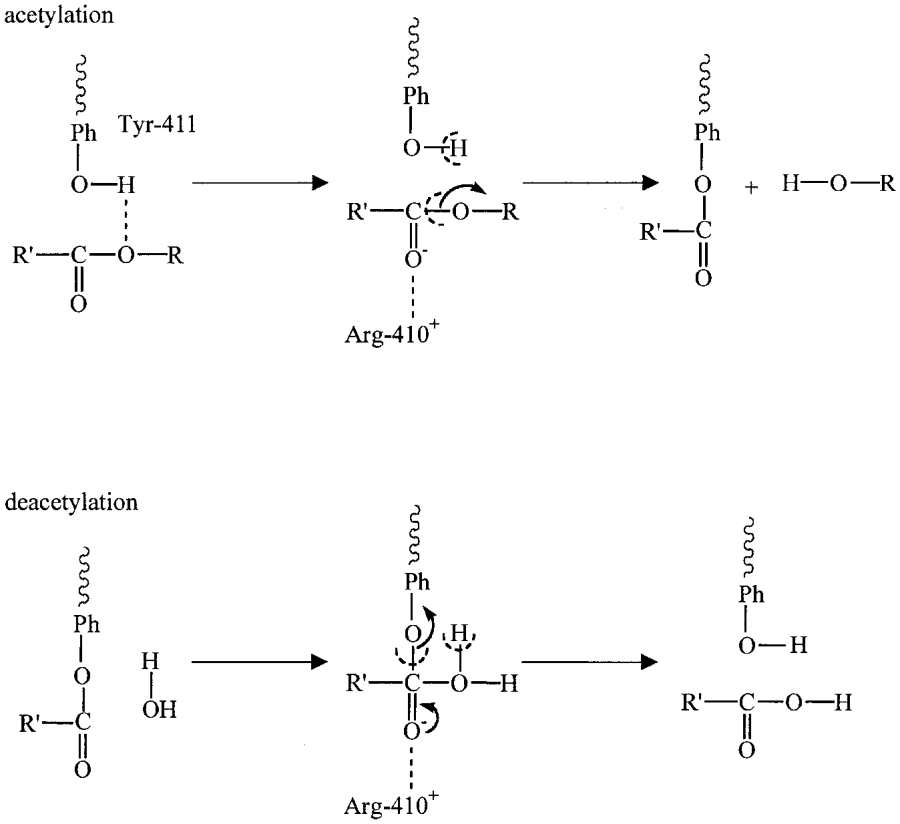

Fig. 5. Simulated mechanism for the hydrolysis of PNPP by HSA.

(16) (Fig. 4). The *p*-nitrophenyl moiety of PNPP is bound to the hydrophobic pocket of MYR-1004 in the X-ray structure. In addition, the *p*-nitrophenyl moiety is associated with the aromatic residues of Tyr-411 and Phe-488. The hydrogen bond between the hydroxyl group of Ser-489 and the carboxyl oxygen atom of PNPP stabilizes the complex. The ethyl moiety of PNPP is bound to a part of the hydrophobic pocket for MYR-1003 in the X-ray structure. The distance between the phenoxyl oxygen atom of Tyr-411 and the carbonyl carbon atom of PNPP was found to be about 3.8 Å and might enable a nucleophilic reaction. The side chain of Arg-410 forms a hydrogen bond with the carbonyl oxygen atom of PNPP, and this hydrogen bond could function as an oxyanion hole. Moreover, The distance between the phenoxyl oxygen atom of Tyr-411 and the carbonyl oxygen atom of PNPP was about 2.8 Å, thus favoring a hydrogen bond formation. This hydrogen bond could account for isotope effect observed for the acetylation of HSA (Fig. 5). This model is consistent with the experimental results; that is, Tyr-411 as the catalytic residue (2,10) and the importance of Arg-410 (10), as mentioned above.

ACKNOWLEDGMENTS

This work was supported in part by Grant-in-Aid for scientific research from the Ministry of Education, Science, and Culture of Japan (11694298 for M.O.) and was also supported in part by Grant-in-Aid for scientific research, encouragement of young scientists (B) (13771414 for N.Y.) from Japan Society for the Promotion of Science.

REFERENCES

1. T. Peter Jr. *All About Albumin, Biochemistry, Genetics, and Medical Applications*, Academic Press, San Diego, 1996.
2. G. E. Means and M. L. Bender. Acetylation of human serum albumin by p-nitrophenyl acetate. *Biochemistry* **14**:4989–4994 (1975).
3. M. A. Sogorb, A. Monroy, and E. Vilanova. Chicken serum albumin hydrolyzes dichlorophenyl phosphoramidates by a mechanism based on transient phosphorylation. *Chem. Res. Toxicol.* **11**:1441–1446 (1998).
4. K. Ikeda and Y. Kurono. Enzymatic activity and drug binding activity of human serum albumin. *Yakugaku Zasshi* **106**:841–855 (1986).
5. C. Y. Quon, K. Mai, G. Patil, and H. F. Stampfli. Species differences in the stereoselective hydrolysis of esmolol by blood esterases. *Drug Metab. Dispos.* **16**:425–428 (1988).
6. T. Satoh, M. Hosokawa, R. Atsumi, W. Suzuki, H. Hakusui, and E. Nagai. Metabolic activation of CPT-11, 7-ethyl-10-[4-(1-piperidino)-1-piperidino] carbonyloxycamptothecin, a novel antitumor agent, by carboxylesterase. *Biol. Pharm. Bull.* **17**:662–664 (1994).
7. A. Awad-Elkarim and G. E. Means. The reactivity of *p*-nitrophenyl acetate with serum albumin. *Comp. Biochem. Physiol.* **91B**:267–272 (1988).
8. X. M. He and D. C. Carter. Atomic structure and chemistry of human serum albumin. *Nature* **358**:209–215 (1992).
9. J. X. Ho, E. W. Holowachuk, E. J. Norton, P. D. Twigg, and D. C. Carter. X-ray and primary structure of horse serum albumin (Equus caballus) at 0.27-nm resolution. *Eur. J. Biochem.* **215**:205–212 (1993).
10. H. Watanabe, S. Tanase, K. Nakajou, T. Maruyama, U. Kragh-Hansen, and M. Otagiri. Role of Arg-410 and Tyr-411 in human serum albumin for ligand binding and esterase-like activity. *Biochem. J.* **349**:813–819 (2000).
11. R. F. Chen. Removal of fatty acids from serum albumin by charcoal treatment. *J. Biol. Chem.* **242**:173–181 (1967).

12. Y. Kurono, T. Maki, T. Yotsuyanagi, and K. Ikeda. Esterase-like activity of human serum albumin: structure-activity relationships for the reactions with phenyl acetates and *p*-nitrophenyl esters. *Chem. Pharm. Bull.* **27**:2781–2786 (1979).
13. N. Ohta, Y. Kurono, and K. Ikeda. Esterase-like activity of human serum albumin II: reaction with N-*trans*-cinnamoylimidazoles. *J. Pharm. Sci.* **72**:385–388 (1983).
14. A. Fersht. *Structure and Mechanism in Protein Science*, Freeman, New York, 1998.
15. H. Tsujishita and S. Hirono. CAMDAS: an automated conformational analysis system using molecular dynamics. Conformational analyzer with molecular dynamics and sampling. *J. Comput. Aided Mol. Design* **11**:305–315 (1997).
16. M. Clark, R. D. Cramer III, and N. Van Opdenbosch. Validation of the general purpose Tripos 5.2 force field. *J. Comp. Chem.* **10**:982–1012 (1989).
17. S. Curry, H. Mandelkow, P. Brick, and N. Franks. Crystal structure of human serum albumin complexed with fatty acid reveals an asymmetric distribution of binding sites. *Nature Struct. Biol.* **5**:827–835 (1998).
18. SYBYL 6.6.2, Tripos Inc., St. Louis, MO, 2000.
19. S. J. Weiner, P. A. Kollman, D. T. Nguyen, and D. A. Case. An all atom force field for simulations of proteins and nucleic acids. *J. Comp. Chem.* **7**:230–252 (1986).
20. J. Gasteiger and M. Marsili. Iterative partial equalization of orbital electronegativity—a rapid access to atomic charges. *Tetrahedron* **36**:3219–3228 (1980).
21. M. Marsili and J. Gasteiger. *Croat. Chem. Acta* **53**:601–614 (1980).
22. J. Gasteiger and M. Marsili. Prediction of proton magnetic resonance shifts: the dependence on hydrogen charges obtained by iterative partial equalization of orbital electronegativity. *Organ. Magn. Reson.* **15**:353–360 (1981).
23. W. P. Purcell and J. A. Singer. A brief review and table of semiempirical parameters used in the Hüeckel molecular orbital method. *J. Chem. Eng. Data* **12**:235–246 (1967).
24. UNITY 4.1.2, Tripos Inc., St. Louis, MO, 2000.
25. G. P. Ford and B. Wang. New approach to the rapid semiempirical calculation of molecular electrostatic potentials based on the AM1 wave function: Comparison with *Ab Initio* HF/6-31G* results. *J. Comp. Chem.* **14**:1101–1111 (1993).
26. B. Wang and G. P. Ford. Atomic charges derived from a fast and accurate method for electrostatic potentials based on modified AM1 calculations. *J. Comp. Chem.* **15**:200–207 (1994).
27 CS ChemOffice Ultra 2000 Enhanced 5.5, CambridgeSoft, Cambridge, MA, 2000.
28. M. Dockal, D. C. Carter, and F. Ruker. Conformational transitions of the three recombinant domains of human serum albumin depending on pH. *J. Biol. Chem.* **275**:3042–3050 (2000).
29. C. Branden and J. Tooze. *Introduction to Protein Structure*, Garland Publishing, Inc., New York, 1991.
30. R. L. Stein. Catalysis by human leukocyte elastase: substrate structural dependence of rate-limiting protolytic catalysis and operation of the charge relay system. *J. Am. Chem. Soc.* **105**:5111–5116 (1983).